Blast Waves Generated by Planar Detonations

P.A. Thibault and J.D. Penrose

Combustion Dynamics Ltd.
Medicine Hat, Alberta Canada

J.E. Shepherd

Department of Mechanical Engineering
Aeronautical Engineering and Mechanics
Rensselaer-Polytechnic Institute
Troy, New York, U.S.A.

W.B. Benedick

Sandia National Laboratories
Albuquerque, New Mexico, U.S.A.

D.V. Ritzel

Defence Research Establishment (Suffield)
Ralston, Alberta, Canada

This paper presents experimental and theoretical studies of blast waves generated by gaseous and HE detonations in long cylindrical tubes. The experimental studies were performed using the 1.8 m diameter shock tube facilities at the Defence Research Establishment Suffield and at the New Mexico Engineering Research Institute. Two gaseous explosives, acetylene-oxygen and hydrogen-air, and one solid explosive, 120g nitroguanidine, were used in order to verify the validity of energy scaling in the far-field. The above experimental work is supported by one- and two-dimensional numerical computations which are based on the Flux Corrected Transport (FCT) algorithm. In the far-field, the experimental results are also analyzed in terms of a simple analytical blast model.

Introduction:

The hazards associated with accidental fuel-air explosions has motivated numerous experimental and theoretical studies on the blast properties of gaseous detonations. It should be noted that most of these studies have focussed on unconfined geometries such as spherical or so-called 'pancake shaped' clouds, whereas very little attention has been given to confined geometries such as ducts, pipes and corridors. This situation is somewhat unfortunate since the latter geometries are, in fact, far more likely sites for deflagration to detonation transition. Furthermore, the recent popularity of gaseous detonation-driven shock tubes for large scale blast simulation has necessitated a much better general understanding of confined detonations with a particular emphasis on planar detonations in long tubes.

General Considerations and Methodology:

As illustrated in figure 1a, the blast wave generated by the detonation of a combustible cloud inside a channel may be expected to vary considerably depending on the size and shape of the cloud, the site of detonation initiation and the distance downstream. Generally speaking, one may divide the blast development into three regimes: 1) a near-field regime involving shock reflections and, hence, a multi-dimensional blast, 2) an intermediate-field regime in which the transverse waves subside and a truly one-dimensional blast wave emerges, and 3) a far-field regime where the blast properties depend solely on the energy released during the detonation.

In order to obtain a better understanding of the parameters involved, experimental studies were performed using 1.8 m diameter shock tube facilities at the Defence Research Establishment Suffield (DRES) and at the New Mexico Engineering Research Institute (NMERI). As illustrated in figures 1b and 1c, the two facilities were similar in scale but differed in that the charge was located at the middle of the NMERI tube which is open at both ends, whereas detonation was initiated at the closed end of the DRES tube. The large scale of these facilities was essential to the present study in order to avoid boundary layer effects which may have influenced previous small-scale experiments [2,3].

The experiments at the DRES facility were performed using acetylene-oxygen balloons .5m, .7m and .9m in diameter which, wnen detonated, delivered an effective energy release of .26, .72 and 1.79 MJ respectively. The experiments at NMERI, on the other hand, consisted of two trials, one using a nitroguanidine (NQ) charge and the other involving the detonation of a bag filled with stoichiometric hydrogen-air. The 120g NQ charge used in the first trial was 25 mm in diameter, 300mm in length and suspended 480 mm from the floor. The bag used in the other trial was .35 m in diameter, 1.2 m long and contained 85g of hydrogen-air which was detonated with 30g of Detasheet explosive. Based on the specific blast energy of the explosives used, both trials involved an energy release of .34 MJ.

In order to examine the full spectrum of near-, intermediate- and far-field effects, the above experimental work was supported by one- and two-dimensional computations based on the Flux Corrected Transport (FCT) algorithm of Boris [3], and by a simple acoustic model.

Near-Field Regime:

Near field effects were observed in all experiments due to the use of point initiation and non-planar cloud geometries. As illustrated in fig. 2, which compares 3 pressure histories for the hydrogen-air and NQ charges in the NMERI tube, these effects resulted in very strong oscillations which, in the case of the NQ charge, were extremely persistent in the near-field and comparable in amplitude to that of the incident blast. Due to the different charge geometries and explosives used in these particular trials, the two signatures are initially very different both in terms of their amplitude and frequency of oscillation. Further downstream, the oscillations decay and the two traces gradually assume a similar behaviour as can be seen from the from the pressure records at 22m. The negative phase observed in the pressure history at this position is due to the expansion wave generated when the shock emerges from the open end of the tube. From the 7 positions monitored along the tube, it would appear that near-field effects, in these particular experiments, persist for approximately 5-10 tube diameters.

The above trials are clearly characterized by very large aspect ratios l/d and D/d which are undoubtedly partly responsible for the large oscillations observed in the pressure records. In order to further explore the nature and extent of the near-field regime, two-dimensional calculations were performed for a cylindrical charge of fuel-air mixture in a circular tube with aspect ratios $l/d = D/d = 2$ (fig. 1-d). The calculation was performed by initiating a planar detonation at the closed end of the cylindrical charge. The detonation was then allowed to propagate freely along the charge using a simple burning model which released energy over approximately 3 grid points. The computation was performed using the FCT algorithm and a grid resolution of 25 grid points per tube radius.

As seen from figure 3a, which shows the pressure profile just after the detonation has reached the end of the charge, the first observed near-field effect is the reflection of the laterally transmitted shock wave off the tube wall and the subsequent interaction of the reflected wave with the burned product contact surface. This, in turn, results in a transmitted shock which implodes onto the axis and an expansion wave which travels back towards the wall. As can be seen from the subsequent profiles, these repeated reflections at the wall, axis and contact surface, not only result in strong oscillations but also in Rayleigh-Taylor instabilities which violently deform the contact surface so as to eventually breakup the volume of burned gas into distinct pockets. The oscillations significantly affect the magnitude of the peak pressure for distances up to approximately $X/D = 8$. After this point, the amplitude of the oscillations gradually decrease and are simply superimposed on an asymptotically decaying pressure profile which, as seen in the following section, is characteristic of the one-dimensional blast wave from a planar detonation.

Intermediate-Field Regime:

Once the transverse waves have sufficiently decayed, the charge shape effects disappear and the pressure signature depends only on the effective charge

length L_c = volume/$\pi D^2/4$ and detonation properties of the mixture. In this regime, the blast properties for a given mixture may be described by defining the appropriate dimensionless distance, time, pressure and impulse as $X^* = X/L_c$, $t^* = C_o t/L_c$, $P^* = \Delta P/P_o$ and $I^* = IC_o/L_c P_o$ where P_o and C_o denote the ambient pressure and sound speed respectively.

The blast properties may be obtained using one-dimensional numerical computations such as those presented by Voitov et al. [4] for planar propane-air and acetylene-oxygen detonations. Since those results were limited to peak pressures over a distance of 10 L_c, additional FCT calculations were performed in order to obtain both pressure and impulse data over an extended domain of 100 L_c. The calculations were performed by imposing the appropriate detonation conditions at the detonation front. The specific heat ratio in the burned products was assigned a pressure dependence corresponding to the equilibrium isentrope passing through the CJ point as obtained from the Gordon-McBride [5] chemical equilibrium code. The grid resolution ranged between 100 to 20 grid points per charge length, L_c ,for distances $X < 10\ L_c$ and $X > 10\ L_c$ respectively.

As seen from figure 4, the calculations indicate that the shock pressure gradually decreases until it reaches a position approximately 5 L_c downstream at which point a temporary plateau is established. This plateau is a consequence of the absence of area expansion in the planar geometry and is not observed in either cylindrical or spherical calculations which are also shown for the sake of comparison. The pressure profiles shown in figure 5 indicate that the plateau is the result of a flat shock which is generated from the tail of Taylor wave in the burned products. The plateau persists until it is completely eroded by an expansion wave which eventually catches up to the leading shock. After this point, the shock strength decays monotonically and the pressure distribution rapidly adopts an asymptotically decaying profile. In fact, the entire one- dimensional shock decay from planar detonations is so gradual that no negative phase is ever observed in the pressure profiles.

As seen from figure 4, the absence of a negative phase also has a drastic effect on the positive impulse properties of planar detonations. Indeed, unlike spherical and cylindrical blasts which decrease in impulse with increasing distance, the widening of the pressure pulse in planar blasts more than compensates for the relatively slow shock decay so as to result in an impulse which has only a very weak dependence on the distance downstream.

Far-Field Regime:

The intermediate-field regime is essentially terminated when the dependence of the blast properties, such as peak pressure and impulse, on the charge length L_c and total combustion energy E_c may be reduced to a function of the latter alone. The ensuing far-field regime may then be described by normalizing the blast data in terms of the so called explosion length (or radius) which is defined as $L_e = (E_c/P_o)^{1/\alpha}$ where α = 1,2,3 for planar, cylindrical and spherical geometries respectively.

Following the convention used by Moen et al. [6] for spherical detonations, the energy E_c may itself be defined as $E_c = \rho_i VQ$ where ρ_i and V denote the initial density and volume of the detonable cloud and Q represents the energy released per unit mass of mixture which, in turn is defined as the difference in enthalpies, at ambient temperature, between the reactants and the burned products. For stoichiometric propane-air, hydrogen-air and acetylene-oxygen mixtures, considered in the present study, the corresponding values of Q derived from the Gordon McBride equilibrium code are 2290, 2818 and 3988 kJ/kg respectively. For a planar charge of length L_c = 1m, these energies translate into explosion lengths of L_e = 27.3, 33.6 and 48.7 m respectively.

The transition between the intermediate- and far-field regime may be examined by re-scaling the numerical results of figure 4 for pressure and impulse in terms of the explosion length L_e. As seen from figure 6, the propane-air and propane-oxygen computations approach each other after the temporary plateau at a

scaled distance $X^* \tilde{=} .3$. It is also interesting to note that, in spite of the two-dimensional near-field oscillations observed in the present experiments, the overall blast properties measured are nevertheless reasonably consistent with far-field energy scaling. Finally, it should also be noted that the present results also agree, in the far-field, with the previous studies of Ohyagi et al. [7] for the transmission of a strong detonation-driven blast wave into a low-pressure gas.

Analytical Acoustic Model:

Comparing the numerical and experimental results in figure 6, it would appear that the one-dimensional calculations, if extended further, would fall slightly above the average trend of the far-field experimental data. This is due to the low resolution used for $X/L_c > 10$, which accounts for the 'kink' in the solution at that point (fig. 4). Rather than extending the range and resolution of the calculations, one may complete the analysis either by using an approximate numerical approach such as the Brinkley-Kirkwood method used by Donato [8] and Haverdings [9], or by applying an analytical acoustic model for weak shocks.

Approximating the profile to be triangular in shape with an amplitude ΔP and a width ΔX, the relationship between ΔP and ΔX may, from energy considerations, be approximated as follows:

$$\Delta P \Delta X = 2(\gamma-1)E_c$$

Furthermore, noting that, in the acoustic limit, the trailing edge of the profile travels at the ambient sound speed, the widening of the pressure pulse is given by

$$d(\Delta X)/dt = U_s - C_o$$

where the shock velocity can be obtained from the shock relation

$$\Delta P/P_o = 2\gamma(M_s^2-1)/(\gamma+1)$$

which in turn can be linearized for $M_s-1 \ll 1$. Proceeding in this manner, one then obtains the following simple analytical solution for the shock overpressure

$$\Delta P/P_o = \frac{4\gamma/(\gamma+1)}{[1 + 4\gamma/(\gamma^2-1) \cdot X/L_e]^{\frac{1}{2}}-1}$$

and the acoustic limit $IC_o/P_oL_e = \gamma - 1$ for the impulse. For $X/L_e \gg 1$, the above solution reduces to the acoustic limit given by Pierce [10]. As can be seen from fig 6, this acoustic solution recovers the far-field numerical solution and accurately represents the average trend of experimental pressure data. On the other hand, the predicted impulses fall slightly below the measured values.

Conclusions:

The combined numerical, analytical and experimental work suggests that, for the chemical systems and aspect ratios considered in the present study, the near, intermediate, and far-field regimes for detonations in confined tubes are approximately divided as follows:

Near field:	$X/D_t \lesssim 8$
Intermediate field:	$X/D_t \gtrsim 8$, $X/L_e \lesssim 0.3$
Far field:	$X/L_e \gtrsim 0.3$

A clear distinction between near and intermediate-field behaviours may be observed provided that $L_e/D_t \gg 8/.3 = 27$. For the experiments performed in the present study, $D_t = 1.8$m, $L_e = 1.1$m for the hydrogen-air and nitroguanidine charges, and ranged between 1.2m to 8.6m for the acetylene-oxygen experiments. Since $L_e/D_t < 5$ for all cases considered, intermediate-field phenomena, such as the pressure plateau observed in one-dimensional calculations, were not observed due to the strong reflections and oscillations which characterize the near-field regime. In the far field, it has been shown that the peak pressures may be predicted quite

accurately using a very simple analytical acoustic model.

Acknowledgements:

We would like to thank the personnel at NMERI, Sandia National Laboratories (Albuquerque) and DRES for their valuable help throughout this study.

References:

1. Bjerketvedt, D.B., Sonju O.K., and Moen I.O., 'The Influence of Experimental Condition on the Reinitiation of Detonation Across an Inert Region', Progress in Astronautics and Aeronautics, Vol. 106, 1986.
2. Donato, M., Donato L. and Lee, J.H.: 'Transmission of Detonations Through Composition Gradients', First Spetialist Meeting (International) of the Combustion Institute, Bordeaux, France, 1981.
3. Boris, J.P.. 'Flux-Corrected Transport Modules for Solving Generalized Continuity Equations.' Naval Research Laboratory Memorandum 3237, March 1976.
4. Voitov, A.P., Gel'fand, B.E., Gubin. S.A., Mikhalkin, V.N. and Shargatov,V.A., 'Effect of Composition of a Combustible Gas Mixture on the Parameters of a Plane Shock Wave Generated by an Explosion in Air' Combustion, Explosion, and Shock Waves (FIZIKA GORENIYA I VZRYVA), July 1984.
5. Gordon, S. and McBride,B.J., 'Computer Program for Calculation of Complex Equilibrium Compositions, Rocket Performance, Incident and Reflected Shocks and Chapman-Jouguet Detonations', 1971.
6. Moen, I.O., Thibault, P.A. and Funk, J.W., 'Blast Waves from Non-Spherical Fuel-Air Explosions.', Proceedings of the 8th International Symposium on Military Application of Blast Simulation, Spiez, Switzerland, 1983.
7. Ohyagi, S., Yoshihashi, T. and Hrigaya, 'A Study on Planar Blast Waves Initiated by Gaseous Detonation',I: Estimation of Initiation Energy' Japan Society for Aeronautical and Space Sciences Vol. 33, 1985.
8. Donato, M., 'The Influence of Confinement on the Propagation of Near Limit Detonation Waves' Ph.D. Thesis, McGill University, 1982.
9. Haverdings, W.,' Evaluation of the 2.0 m Diameter Blast Simulator Driven by Fuel-Oxygen Explosive Charges', Proceedings of the 8th International Symposium on Military Application of Blast Simulation, Spiez, Switzerland, 1983.
10. Pierce, A.D., 'Acoustics', McGraw Hill 1981.

Figure 1

EXPERIMENTAL AND COMPUTATIONAL CONFIGURATIONS

A: General Schematic

B: DRES Experiments

C: Sandia-NMERI Experiments

H_2 : AIR ; l = 60 cm , d = 36 cm

NQ ; l = 15 cm , d = 2.5 cm

D: Numerical Computation

C_3H_8 : AIR ; D = 1 = 2d

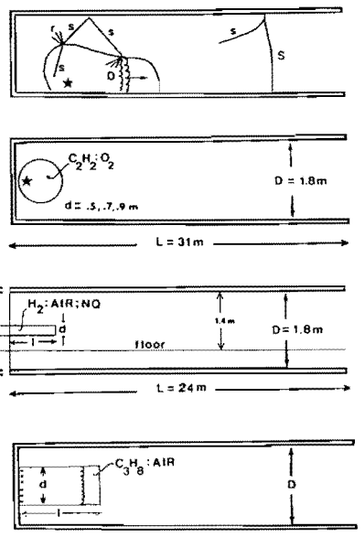

Figure 2

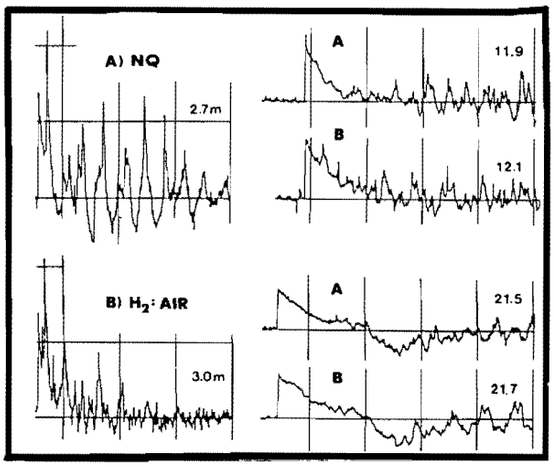

COMPARISON OF PRESSURE RECORDS

A) Nitroguanidine (NQ)
B) H_2:AIR

Vertical and horizontal scales
34.5 kPa / full div.
10 ms / div.

Ambient pressure: 83 kPa

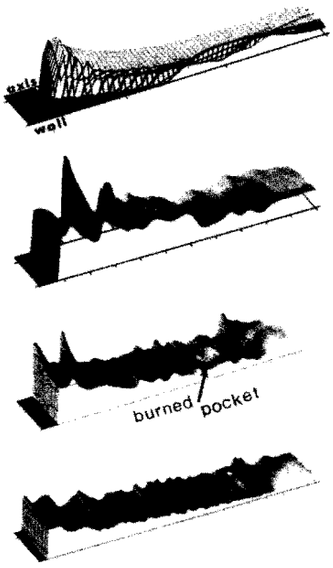

Figure 3

NUMERICAL 2-D COMPUTATIONS

Pressure Profiles: X/D = 1,4,8 13
20 grid points (2D/5) per division

Light regions: burned gas
Dark regions: air

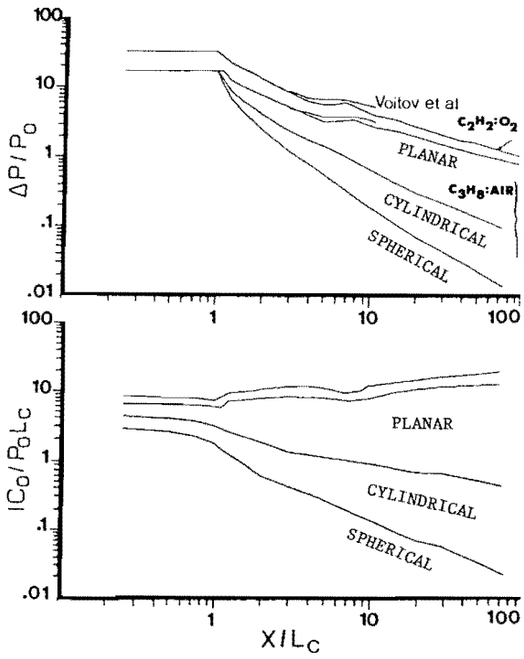

Figure 4

NUMERICAL 1-D COMPUTATIONS

Comparison of Blast Overpressures and Impulses for Planar, Cylindrical and Spherical Detonations.

Figure 5

PRESSURE PROFILE EVOLUTION FOR PLANAR DETONATION

C_3H_8:Air, Vertical amplitude denotes $\log(P/P_o)$

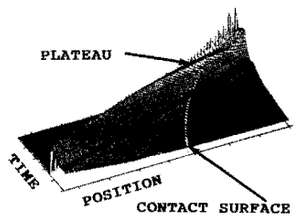

Figure 6

ENERGY SCALED OVERPRESSURES AND IMPULSES FOR PLANAR DETONATIONS

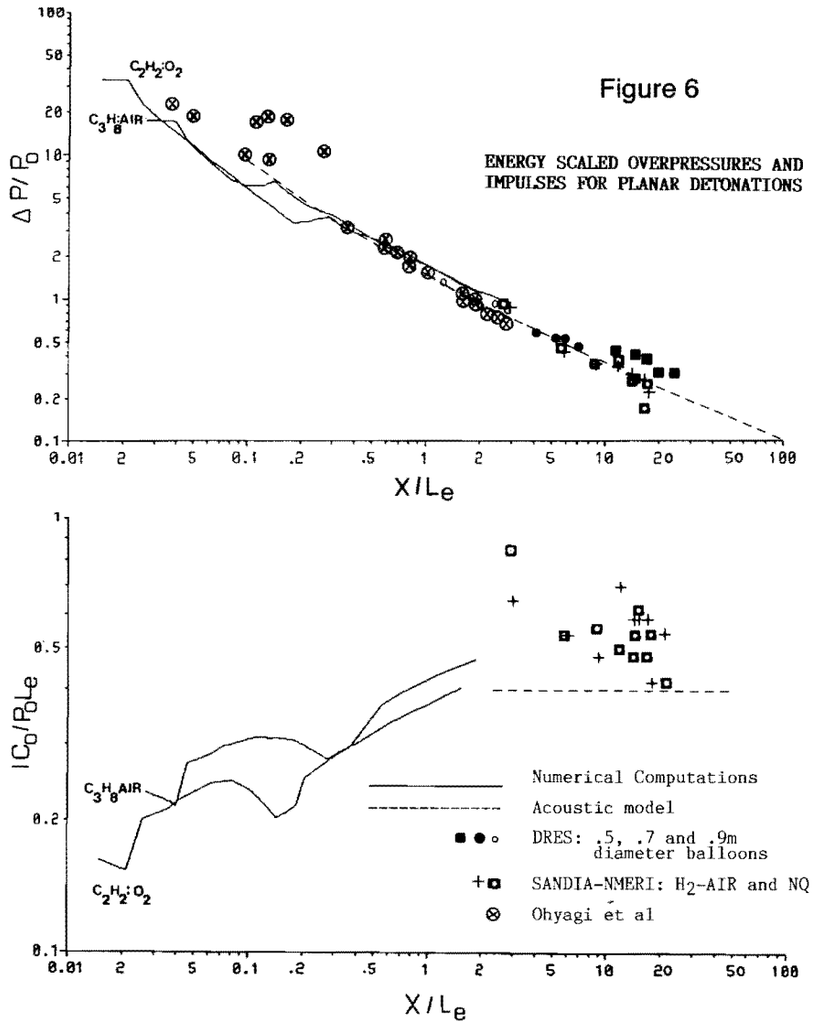

Reprint of

Shock Tubes and Waves

Proceedings of the
Sixteenth International Symposium on
Shock Tubes and Waves
Aachen, West Germany, July 26–31, 1987

edited by
Hans Grönig

Rheinisch-Westfälische
Technische Hochschule Aachen